# Incident energy and polarization-dependent resonant inelastic x-ray scattering study of $La_2CuO_4$

L. Lu,[1] J. N. Hancock,[2] G. Chabot-Couture,[1] K. Ishii,[3] O. P. Vajk,[4] G. Yu,[5] J. Mizuki,[3] D. Casa,[6] T. Gog,[6] and M. Greven[1,2]

[1]*Department of Applied Physics, Stanford University, Stanford, California 94305, USA*

[2]*Stanford Synchrotron Radiation Laboratory, Stanford, California 94309, USA*

[3]*Synchrotron Radiation Research Unit, Japan Atomic Energy Agency, Hyogo 679-5148, Japan*

[4]*NIST Center for Neutron Research, National Institute of Standards and Technology, Gaithersburg, Maryland 20899, USA*

[5]*Department of Physics, Stanford University, Stanford, California 94305, USA*

[6]*CMC-XOR, Advanced Photon Source, Argonne National Laboratory, Argonne, Illinois 60439, USA*

(Received 10 July 2006; published 28 December 2006)

We present a detailed Cu *K*-edge resonant inelastic x-ray scattering (RIXS) study of the Mott insulator $La_2CuO_4$ in the 1–7 eV energy loss range. As initially found for the high-temperature superconductor $HgBa_2CuO_{4+\delta}$, the spectra exhibit a multiplet of weakly dispersive electron-hole excitations, which are revealed by utilizing the subtle dependence of the cross section on the incident photon energy. The close similarity between the fine structures for in-plane and out-of-plane polarizations is indicative of the central role played by the 1*s* core hole in inducing charge excitations within the $CuO_2$ planes. On the other hand, we observe a polarization dependence of the spectral weight, and careful analysis reveals two separate features near 2 eV that may be related to different charge-transfer processes. The polarization dependence indicates that the 4*p* electrons contribute significantly to the RIXS cross section. Third-order perturbation arguments and a shake-up of valence excitations are then applied to account for the final-energy resonance in the spectra. As an alternative scenario, we discuss fluorescence-like emission processes due to $1s \rightarrow 4p$ transitions into a narrow continuum 4*p* band.

DOI: 10.1103/PhysRevB.74.224509 PACS number(s): 74.25.Jb, 74.72.−h, 78.70.Ck, 71.35.−y

## I. INTRODUCTION

With the advent of third-generation synchrotron sources, inelastic x-ray scattering has emerged as a powerful probe of momentum- and energy-dependent charge and lattice dynamics. This development has led to new insight into low-density metallic electrodynamics,[1] valence fluctuating compounds,[2] $H_2O$ molecular correlations,[3,4] phonon dynamics,[5] and the Mott physics of correlated electron systems such as the lamellar copper oxides[6–14] and the manganites.[15,16] Resonant inelastic x-ray scattering (RIXS) provides a considerable advantage over ordinary inelastic scattering since, at resonance, the inelastic signal is significantly enhanced.[17] In the lamellar copper oxides, this resonance condition can be readily met by tuning the incoming photon energy to the vicinity of the Cu *K* edge. The RIXS cross section sensitively depends on the incident photon energy and on the nature of the intermediate states.[12,18–20]

If viewed as a two-stage process, the intermediate state in RIXS is the same as the final state of x-ray absorption: for example, in Cu *K*-edge RIXS, a localized core hole is created through $1s \rightarrow 4p$ photoexcitation. The 1*s* core hole interacts strongly with the valence electron system, generating a strong response that corresponds to the many-electron bound states of the local, nascent core-hole potential.[21] In RIXS, the relaxation of these highly excited states leads to the emission of photons and leaves the valence system in an excited state. One usually identifies energy-loss features with the excitations of the valence electrons. When viewed as a second-order optical process, there exists a close connection between the initial absorption and final emission stages in RIXS. Accordingly, the spectra simultaneously depend on both the incident and final photon energies.[22]

In the present work, we investigate these energy dependences as well as the polarization dependence of the cross section in $La_2CuO_4$, the best-characterized lamellar copper oxide. This Mott insulator is the parent compound of the original high-temperature superconductor $(La,Ba)_2CuO_4$, and it has been the subject of a number of prior RIXS studies.[10,12,23] Exploiting the incident-energy sensitivity, we are able to identify additional charge excitation features. We demonstrate that the fine structure is present for photon polarization both parallel and perpendicular to the $CuO_2$ planes, and suggest that the subtle differences between the two polarization conditions can be explained in terms of models in which the 4*p* electrons play a significant role.

This paper is organized as follows. After the discussion of the experimental details in the next section, we present our results for out-of-plane and in-plane polarization in Secs. III and IV, respectively. Section V contains a discussion of our data, and we summarize our work in Sec. VI.

## II. EXPERIMENTAL DETAILS

The focus of this work is on the collective electronic excitations of $La_2CuO_4$ in the 1–7 eV range using incident photon energies in the vicinity of the Cu *K*-edge absorption threshold. We have measured the RIXS response at several high-symmetry positions in the Brillouin zone, covering a fine mesh of incident and scattered photon energies around the Cu *K* edge.

Two sets of measurements were taken, one collected at the Advanced Photon Source with incident photon polarization vector perpendicular to the $CuO_2$ planes ($\mathbf{E} \| c$), and the other at SPring-8 (Japan) with incident photon polarization

 

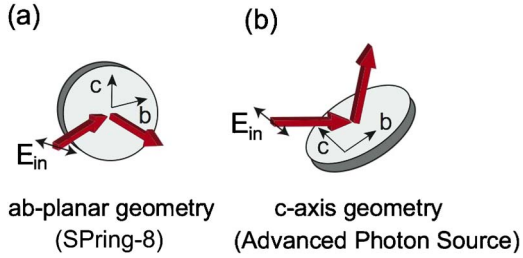


FIG. 1. (Color online) The two scattering geometries used in this study and discussed in the text.

parallel to the $CuO_2$ planes ($\mathbf{E} \perp c$). The measurements with in-plane polarization [Fig. 1(a)] were taken in horizontal scattering geometry at beamline BL11XU at SPring-8, with the tetragonal reciprocal lattice point $\mathbf{G}=(3,0,0)$ as Brillouin zone center, and a scattering angle of ~65°. A Si(111) main monochromator and a Si(400) secondary monochromator were used to obtain an incident energy resolution of 220 meV. A bent Ge(733) analyzer crystal situated at the end of a 2 m four-circle diffractometer arm selected the energy of the photons scattered from the sample, which were then collected by a solid state detector. In this geometry, the polarization vector of the incident photon was always parallel to the $CuO_2$ planes, with a typical angle of ~32° with respect to the tetragonal *a* axis, i.e., the planar Cu-O bond direction. The overall energy resolution was about 400 meV [full width at half maximum (FWHM)], as determined from the energy width of the elastic line.

Out-of-plane polarization measurements [Fig. 1(b)] were performed at beamline 9-ID-B at the Advanced Photon Source in a vertical scattering geometry. The reciprocal lattice vectors (3,0,0) and (1,0,0) were chosen as reference zone centers to reduce the contribution from the elastic tail, because Bragg scattering at these reflections is forbidden. The setup employed a Si(111) primary monochromator, a Si(333) secondary monochromator, and a spherical diced Ge(733) analyzer crystal with a 1 m radius, and yielded an overall energy resolution of about 300 meV (FWHM). For data collected that were measured at the reduced wave vector $(\pi,0)$, or absolute momentum of (1.5,0,0), we used a primary Si(111) and a second Si(444) channel-cut monochromator in conjunction with a diced analyzer on a 2 m diameter Rowland circle. This configuration can provide at best an energy resolution of 110 meV, but we chose wide aperture slits in front of the detector to obtain a significant signal boost and a comparable resolution of ~300 meV for better comparison with measurements at other wave vectors.

Data were taken at ambient temperature on the same single-crystalline sample in both polarization geometries. $La_2CuO_4$ undergoes a tetragonal-to-orthorhombic structural phase transition at ~530 K associated with the staggered tilting of the $CuO_6$ octahedra.[24] We note that our crystal is twinned, and hence we do not distinguish between the two inequivalent planar orthorhombic directions. The crystal was grown in an image furnace at Stanford University. As-grown crystals are known to contain excess oxygen, and hence hole carriers. In order to assure that the sample was free of any carriers it was annealed for 24 h in Ar flow at 950 °C. This reduction treatment resulted in a Néel temperature of $T_N$ ~320 K, as determined from a measurement of the magnetic susceptibility.[25]

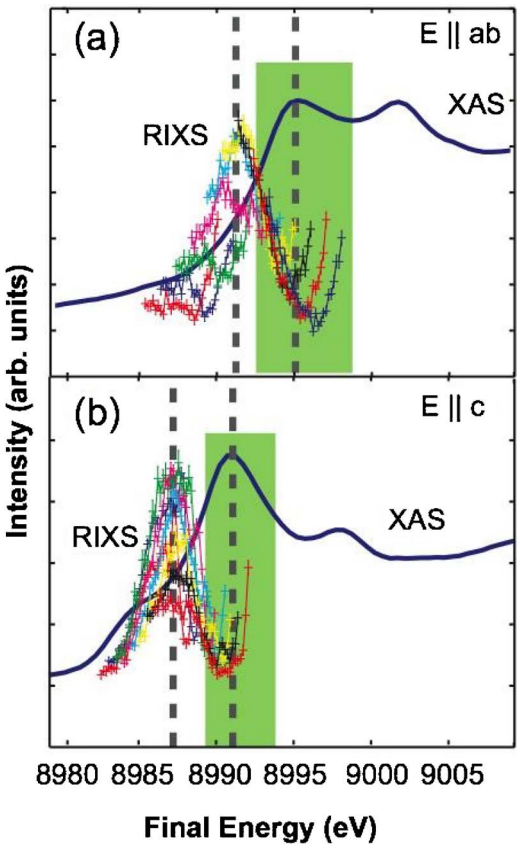


FIG. 2. (Color online) RIXS spectra plotted versus final photon energy along with the absorption spectra monitored by total fluorescence yield for photons polarized (a) parallel and (b) perpendicular to the $CuO_2$ planes. The shaded areas indicate the incident-energy ranges probed in the present study. All spectra were taken at $\mathbf{Q}=(3,0,0)$ and at different incident energies corresponding to the shaded ranges.

Figure 2 shows the x-ray absorption spectra (XAS) for each polarization condition as measured by total fluorescence yield. For each polarization, there are two peaks, at 8991 and 8998 eV for $\mathbf{E} \| c$, and at 8995 and 9002 eV for $\mathbf{E} \perp c$. The lower of these resonances is usually identified with a transition into a "well-screened state,"[6,8,10] a many-body excitation which effectively screens the 1*s* core hole and has significant $1\underline{s}4p3d^{10}\underline{L}$ character. The higher resonance is identified with a transition into a "poorly screened state,"[6,8,10] another bound state of the many-electron system in the core hole potential which has predominantly $1\underline{s}4p3d^9$ character. For each polarization, the resonance peaks are separated by approximately 7 eV. The resonance energies differ by about 4 eV between the two geometries, which may be primarily due to the larger Cu-O distance for the negatively charged apical oxygens, rendering the $4p_z$ electronic orbitals lower in energy than their $4p_\sigma$ counterparts.[26,27] The spectra presented in this paper were taken in the vicinity of the well-screened condition for both polarization geometries.

### III. INCIDENT-ENERGY DEPENDENCE, OUT-OF-PLANE POLARIZATION

RIXS spectra obtained in early work in the soft x-ray regime exhibited a clear incident and final photon energy dependence.[22] The incident-photon-energy dependence was recently employed in the hard x-ray regime (at the Cu $K$ edge) in a study of both $La_2CuO_4$ and the single-layer high-temperature superconductor $HgBa_2CuO_{4+\delta}$ (Hg1201).[12] This study revealed additional features in the 2–5 eV range, an observation that necessitates a new interpretation of the charge dynamics in these materials. For example, a ~2 eV feature was identified in Hg1201. It was argued in Ref. 12 that this feature is not likely a $d \rightarrow d$ excitation, but rather indicates the presence of a remnant charge-transfer gap even at optimal doping in this model superconductor. The presence of an additional feature at ~3 eV, which was only identified through inspection of multiple spectra obtained with different photon energies, constrains the dispersion of the 2 eV feature to be less than 500 meV. The same approach was applied to $La_2CuO_4$, and preliminary data revealed charge-transfer features that are remarkably similar to those in Hg1201,[12] a result that is qualitatively different from prior work on the Mott insulators $La_2CuO_4$ (Ref. 10) and $Ca_2CuO_2Cl_2$.[9] The small dispersion of the 2 eV feature was further confirmed by subsequent measurements.[23,28] Our primary focus here is to investigate in greater detail the incident-energy and polarization dependence of the inelastic cross section near the absorption threshold in $La_2CuO_4$.

The molecular orbital excitation at ~7 eV was studied in detail in Ref. 11 and is most prominently observed near $E_i$ =8998 eV, an incident photon energy for which the lower-lying charge-transfer excitations in the 2–6 eV range do not resonate. We therefore limit our attention to the incident energy range $E_i$=8989–8994 eV [shaded area in Fig. 2(b)] and to energy transfers below 7 eV for out-of-plane polarization. A fine step size of $\Delta E_i$=500 meV was chosen, allowing us to demonstrate the high sensitivity of the RIXS cross section to the incident photon energy.

Figure 3(a) shows representative line scans at the zone center, taken at three different incident energies with out-of-plane polarization. These data resemble previous work,[10] yet closer inspection reveals additional features. At low incident energy, the most distinct feature is that at 2.25 eV. As the incident energy is increased, this sharp feature gradually weakens relative to those at higher energy. A new feature at 3 eV, which was not observed in prior work,[10] can be discerned at all three incident photon energies. The feature at ~4 eV, also seen in previous zone-center data. Finally, a comprehensive analysis of all data[12] reveals a second additional feature at ~5 eV. We discuss below how the systematic center-of-mass shift with incident energy suggests a modulation of the inelastic cross section through final photon-energy-dependent denominators.

Figure 3(b) shows a contour plot constructed from all line scans at the zone center. This mode of representation is similar to the "RIXS plane" of incident photon energy versus energy transfer in Ref. 29. By extending the energy-transfer spectra into the incident-energy dimension, the features at ~2.25, 3, and 4 eV are readily apparent.

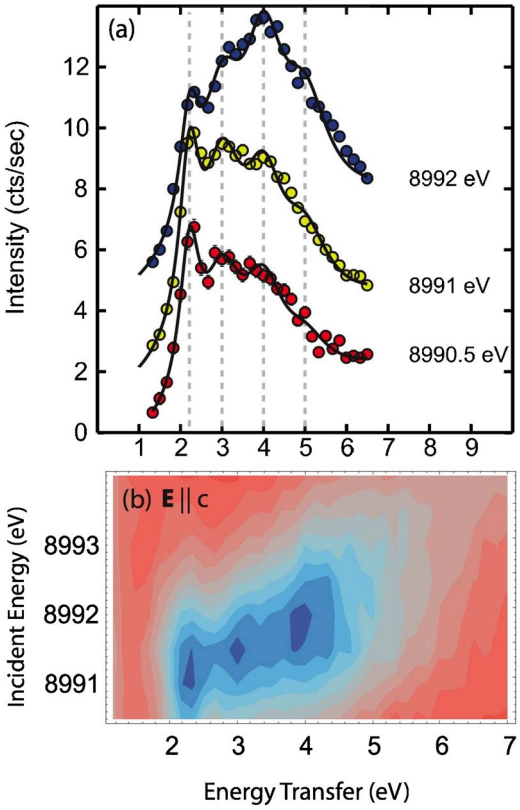


FIG. 3. (Color online) (a) RIXS signal versus energy transfer for out-of-plane polarization at three representative incident energies at a momentum transfer of (3,0,0), which corresponds to the two-dimensional zone center (0,0). The lines are the result of a fit, as discussed in the text (reproduced from Ref. 12). (b) Contour plot of all zone-center scans, taken in 500 meV increments of $E_i$.

Figure 4 shows additional results at high-symmetry points of the two-dimensional Brillouin zone. Using the fit procedure defined in Ref. 12, the spectra at each momentum transfer are fitted simultaneously to obtain the peak positions that determine the energy transfer of the corresponding charge excitations. Specifically, we assume that the peak positions do not vary with incident energy and that each energy-transfer feature is represented by a Lorentzian line shape. The number, energy-transfer positions, and energy widths of the features are considered to be shared parameters for all spectra at the same momentum transfer. At different incident energies, on the other hand, the spectral weight of each component is allowed to vary. We also use spectra on the energy-gain side (not shown in Fig. 4) for background subtraction, and allow for linear slopes to approximate the continuum due to transitions to continuous unoccupied states. A simultaneous least-squares fit of all spectra at each momentum transfer results in the lines in Figs. 3(a) and 4 and allowed us to extract the peak positions plotted in Fig. 5.

Although the different components are not as easily distinguishable as at the zone center, the relative strengths of the four features identified below 6 eV exhibit distinct dependences on momentum transfer and incident energy, which may be indicative of different excitation symmetry. The 5 eV component is most pronounced at $(\pi,\pi)$ and at relatively high incident energies. Away from the zone center, the rela-

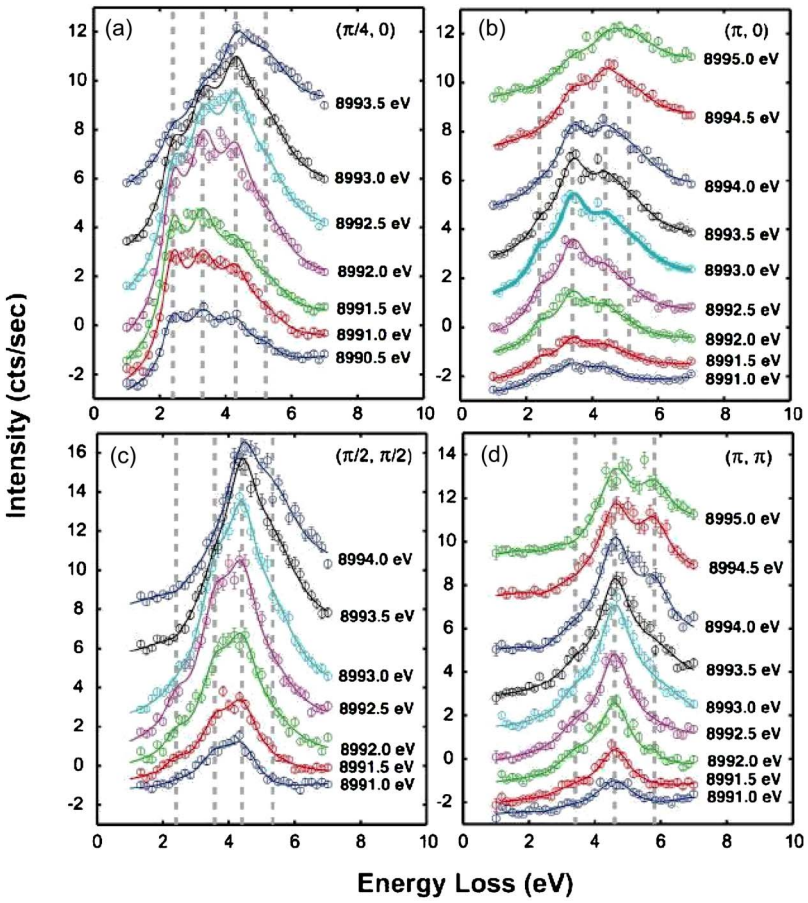


FIG. 4. (Color online) Incident-energy dependence of the $\mathbf{E}\|c$ RIXS spectra for (a) $(\pi/4,0)$, (b) $(\pi,0)$, (c) $(\pi/2,\pi/2)$, and (d) $(\pi,\pi)$. The lines are the result of fits, as discussed in the text.

tive weight of the 2 eV feature quickly decreases. While the 2 and 3 eV features are still separable and comparable in strength at $(\pi/4,0)$, the 2 eV component is only barely visible (at low incident energies) at $(\pi,0)$, the 3 and 4 eV features maintain comparable weight along $[\pi,0]$. In contrast, along $[\pi,\pi]$, the overall response away from the zone center appears to be dominated by the (approximately Lorentzian-shaped) response just above 4 eV. As for the fine structure, the momentum dependence away from the zone center is again consistent with what is observed in Hg1201, although that study was carried out with in-plane polarization.[12]

## IV. INCIDENT-ENERGY DEPENDENCE, IN-PLANE POLARIZATION

Figure 6 shows line scans at the zone center for the complementary in-plane-polarized (SPring-8) experiment. As indicated in Fig. 2(b), the incident photon energy was chosen to lie in the range 8993–8999 eV. The fine structure revealed through the incident energy dependence of the spectra is very similar to that found for out-of-plane polarization. Differences in the configuration between the two experiments make a direct comparison of signal levels difficult. Overall, there are still four major features present at ~2, 3, 4, and 5 eV. The close similarity of the spectra supports the intuitive notion that the spherically-symmetric 1*s* core hole potential dominates the generation of the valence excitations in both cases.[9,30–33]

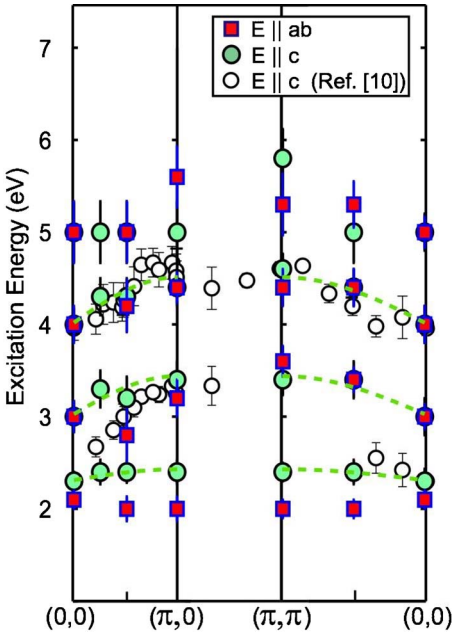


FIG. 5. (Color online) Dispersion of the charge excitations for both in-plane and out-of-plane polarization along the two high-symmetry directions studied in the present work. The dashed lines indicate sinusoidal fits to the dispersion of the three lowest-energy features discerned with out-of-plane polarization. Previous results (Ref. 10), obtained with out-of-plane polarization, are shown for comparison.

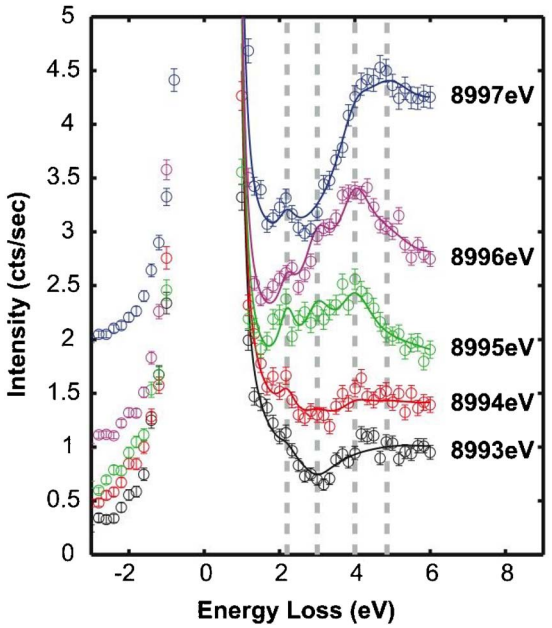


FIG. 6. (Color online) Five line scans at the zone center obtained with in-plane polarization.

There also exist similarities between the two polarization geometries in the momentum dependence of the multiplet structure. Figure 7 shows line scans with fits at four reduced momentum transfer values away from the zone center. As in the out-of-plane polarized experiment, the strength of the 2 eV feature decreases toward the zone boundary. In the present case, it is no longer visually observable at $(\pi,0)$. Also, the 3 and 4 eV features have comparable spectral weight along $[\pi,0]$, and remain comparable up to $(\pi/2,\pi/2)$ along $[\pi,\pi]$. Between $(\pi/2,\pi/2)$ and $(\pi,\pi)$, however, the 3 eV feature is quickly suppressed between and, as in the case of out-of-plane polarization, the 4 eV spectral weight becomes dominant.

Differences between the spectra obtained in the two geometries are also noticeable. First, with in-plane polarization, the intensity of the 2 eV feature relative to that of spectral features with higher energy transfer is much smaller than for the out-of-plane polarized experiment. However, the 2 eV feature is still observable even up to $(\pi,\pi)$, reaching a maximum at an incident energy of 8997 eV, slightly above the absorption threshold (8995 eV) for in-plane polarization. Second, for in-plane polarization, as we increase in incident energy, the center of mass of the spectra continuously shifts to higher energy transfers. For out-of-plane polarization, on the other hand, it peaks between 4 and 5 eV.

As for the $\mathbf{E}\|c$ data, all spectra acquired at the same momentum transfer were simultaneously fit assuming the same set of peak positions. The results of the fits are shown by the lines in Figs. 6 and 7 and the peak positions are compared to those for out-of-plane polarization in Fig. 5. While there is an overall good agreement, the 2 eV features have significantly different excitation energies for the two polarization conditions. We note that the dispersions of all four features summarized in Fig. 5 are weak. These observations will be discussed in more detail in the next section.

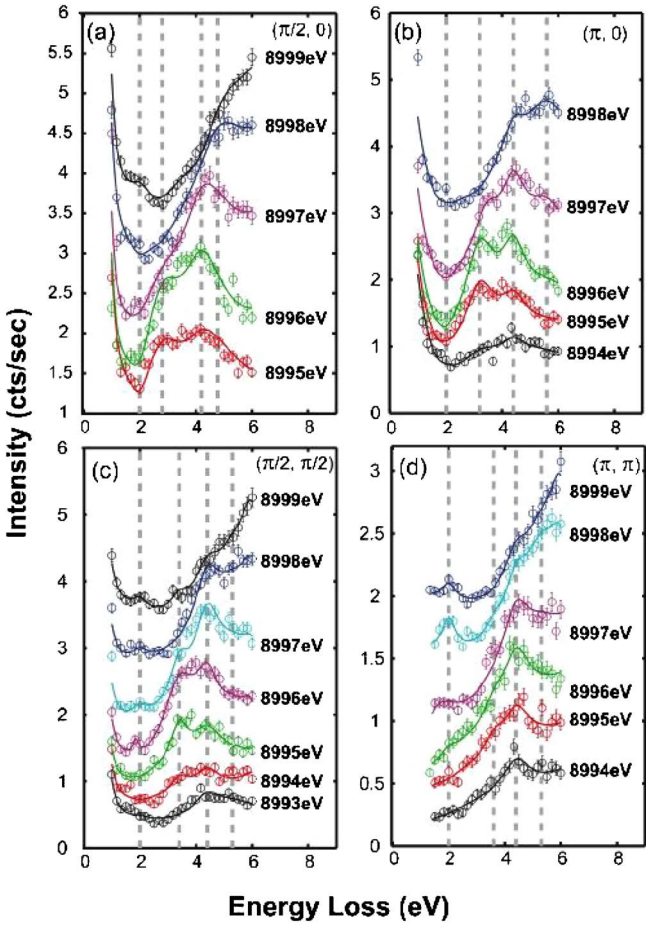


FIG. 7. (Color online) RIXS spectra obtained with $\mathbf{E}\|ab$ at (a) $(\pi/2,0)$ (b) $(\pi,0)$ (c) $(\pi/2,\pi/2)$, and (d) $(\pi,\pi)$.

## V. DISCUSSION

The presence of a ~2 eV resonance feature has been discussed in connection with excitations across the charge transfer gap.[7,9,10,12,22] In $La_2CuO_4$, this excitation is observed only for transitions into well-screened states, in which the 1*s* core hole is screened by a valence electron from a neighboring $CuO_4$ plaquette, leaving a doubly occupied $Cu^+$ ion ($3d^{10}$) and a hole on the neighboring plaquette. It has been suggested that the nonlocal hole can form a Zhang-Rice singlet,[34] which can propagate efficiently through the antiferromagnetic background, and that this singlet could form a strong bond with the $Cu^+$ quasiparticle and become even more dispersive as a bound exciton.[35] However, high-resolution electron-energy-loss spectroscopy (EELS) on the related Mott insulator $Sr_2CuO_2Cl_2$ suggests the existence of another charge-transfer excitation, with slightly lower energy, that involves only the local $CuO_4$ plaquette. These latter findings were argued to be consistent with embedded molecular cluster calculations.[36] Indeed, our data reveal that the actual excitation energies of the 2 meV feature differ by as much as 300 meV for in-plane and out-of-plane polarization conditions. While the former excitation has no discernible dispersion, the latter appears to disperse by 100–150 meV toward the zone boundary. In addition to these differences,

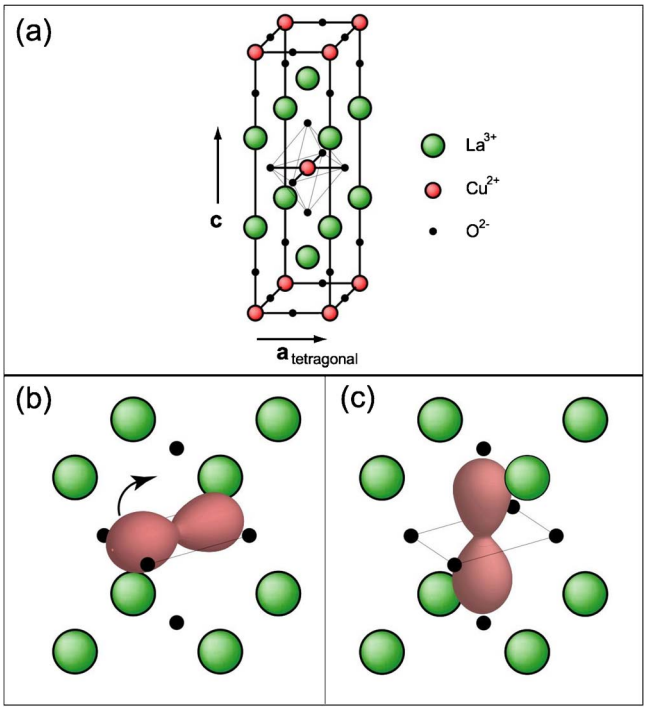


FIG. 8. (Color online) (a) $La_2CuO_4$ unit cell. In a Cu $K$-edge absorption process, several $4p$ states can be reached, depending on the polarization of the incident photon relative to the crystal axes. (b) $4p_\sigma$ configuration created by absorption of a $E_i \sim 8996$ eV photon with $E \| ab$. (c) $4p_z$ configuration created by absorption of a $E_i \sim 8991$ eV photon with $E \| c$. The emissive process discussed in the text corresponds to relaxation from state (b) to state (c).

we also find that the spectral weights of these two low-energy features exhibit rather different momentum dependences, especially along $[\pi, \pi]$. We note that it is not likely that the 2 eV features are $d \rightarrow d$ excitations, since the latter lie below 2 eV and are expected to be much weaker at the $K$ edge than at the $L$ and $M$ edges.[22]

In an attempt to understand the differences between the two 2 eV features, we consider a possible photon polarization effect. When the polarization vector of the incident photon lies within the $CuO_2$ plane, the $4p$ electron in the intermediate state is in the $4p_\sigma$ orbital [see Fig. 8(b)] and overlaps with the $2p_{x,y}$ electrons. The repulsive Coulomb interaction between O $2p$ and Cu $4p$ therefore tends to suppress the O $2p \Rightarrow$ Cu $3d$ charge transfer. On the other hand, for out-of-plane polarization, the $4p_z$ orbital is oriented orthogonal to the $2p_{x,y}$ electrons [see Fig. 8(c)] and the Coulomb interaction has a limited effect on the charge-transfer process. That difference in intermediate states may explain why we observe a second (local) "2 eV" component for in-plane polarization, since the component that involves a nonlocal charge-transfer process from a neighboring $CuO_4$ plaquette to the central core hole site could be spectroscopically suppressed for in-plane polarization. The lower of the two 2 eV features may be intrinsically weaker, which could explain why we are unable to discern it for out-of-plane polarization. As an alternative scenario, consistent with the identification of two distinct features, a detailed analysis of the scattering configurations reveals that the optical-limit Raman efficiencies set by geometry are quite different in each case. It is possible that the suppression of the higher energy feature for the plane-polarized experiment reflects details of the symmetry of this excitation. Further experimentation is required to resolve this possibility. The above is consistent with earlier suggestions based on Cu $K$-edge XAS.[37] Especially for in-plane polarization, the $\sim$2 eV excitation still maintains its strength along $[\pi, \pi]$, whereas it is weakened at the same location for out-of-plane polarization. Therefore, it indeed appears that these two low-energy excitations have a distinct physical origin, consistent with the high-resolution EELS work.[36]

The magnitude of the dispersion will be an important factor in the eventual determination of the origin of the charge excitations. Our $La_2CuO_4$ data reveal charge-transfer features that are remarkably similar to those for Hg1201,[12] a result that is qualitatively different from prior work on $La_2CuO_4$.[10] As summarized in Fig. 5, below 4 eV we identify one additional branch at $\sim$3 eV for both polarization conditions. For example, for out-of-plane polarization, simple fits to a sinusoidal form (shown in Fig. 5) yield dispersions of 120(30), 410(110), and 490(70) meV for the 2, 3, and 4 eV features along both high-symmetry directions. The 5 eV feature is dispersionless within the experimental uncertainly, and we note a possible anomaly at $(\pi, \pi)$. Below, we discuss the possibility that the 5 eV feature may actually be the result of a "shake-up" excitation at 7.2 eV. The $\sim$100 meV dispersion of the nonlocal 2 eV excitation is less than the Zhang-Rice singlet bandwidth of 250 meV identified by angle–resolved photoemission spectroscopy.[38–40] This observation challenges the notion of an excitonic picture to explain the dispersion of the charge-transfer gap excitation. In principle, if the electronic states of the electron and hole are asymmetric,[41] the observed dispersion may either represent the bandwidth of the upper Hubbard band, if the electron is more mobile, or of the Zhang-Rice singlet band, if the hole is freer to move. However, it is difficult to reconcile the small electron-hole-pair dispersion of $\sim$100 meV with the relatively large Zhang-Rice singlet bandwidth, unless the observed behavior represents a significant core hole effect.

In order to understand the appearance of multiple charge excitations in the higher-energy (transfer) region, a more complex approach appears to be necessary. An initial suggestion concerning the 4 eV excitation invoked an excitonic state of unspecified origin,[10] yet more recent work[12,32,42] suggests that the higher-energy spectral features ought to be described in terms of a multiband picture. Considering the involvement of bonding and nonbonding oxygen $2p_\sigma$ and $2p_z$ orbitals, as well as charge-transfer processes through local and nonlocal screening channels, there exist many candidate modes. Eskes and Sawatzky[43] also find that triple-band physics, including the Zhang-Rice triplet states, as well as $d_{3z^2-r^2}$-orbitals are relevant up to about 7 eV in binding energy. Further experimentation, including symmetry analysis, is required to resolve the physical origin of the high-energy spectral features.

We will now discuss the photon energy and polarization dependence of the observed higher-energy features. Figure 9(a) shows zone-center contour plots of incident energy versus energy transfer. The out-of-plane data are from Ref. 10

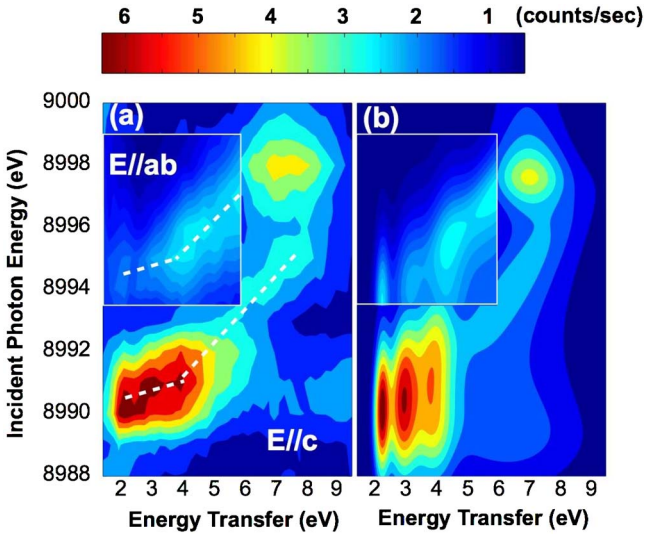


FIG. 9. (Color online) (a) Contour plot of $La_2CuO_4$ RIXS intensity: incident photon energy vs energy transfer for $\mathbf{E}\|c$ (from Ref. 10) and $\mathbf{E}\|ab$ (inset; present work). The white dashed lines indicate the two trends with different slope, as discussed in the text. (b) Calculations following third-order perturbation theory, as discussed in the text.

and were taken with coarser incident energy step size (1 vs 0.5 eV), but span a wider incident energy range than our data in Fig. 3(b). The in-plane data (inset) are from our present study and were taken with incident-energy increments of 1 eV. As mentioned above, the center of mass of the RIXS spectra shifts to higher energy transfer as the incident photon energy increases. This variation is identified in Fig. 9(a) as a "streak" of intensity from 2 to ~7 eV which, instead of extending horizontally as one would expect for resonances associated with fixed incident photon energy, tilts toward the upper right corner. We will first discuss that this streak of intensity can be interpreted in a shakeup picture, which uses third-order perturbation theory. As an alternative scenario for the slope-1 component of this streak of intensity between ~5 and 7 eV, we will then discuss fluorescence-like emission processes due to $1s \rightarrow 4p$ transitions into a narrow continuum $4p$ band.

Pioneering work on $La_2CuO_4$ (Ref. 7) utilized in-plane polarization and revealed one single excitation between ~3 and 6 eV, and it was found that the peak position varied nonlinearly with incident energy. These results were interpreted in terms of a shake-up of the $3d$ electron system, and explained within third-order perturbation theory. Following this treatment, which was formulated in detail in Ref. 7, 19, and 44, the scattering amplitude in third-order perturbation theory is given by

$$A \propto \sum_{m,n} \frac{\langle f|b_2|m\rangle\langle m|H_c|n\rangle\langle n|b_1|i\rangle}{(E_m - E_{f,el} - E_f - i\Gamma_m)(E_n - E_{i,el} - E_i - i\Gamma_n)}$$
$$\approx \frac{\langle f|b_2 H_c b_1|i\rangle}{(E_{ex,2} - E_f - i\Gamma_2)(E_{ex,1} - E_i - i\Gamma_1)} \quad (1)$$

where $|m\rangle$ and $|n\rangle$ denote different intermediate states containing a virtual $1s4p$ exciton, $E_i$ and $E_f$ are the incident and final photon energies, $E_{i,el}$ and $E_{f,el}$ the initial and final energies of the electron system, and $b_1$ and $b_2$ the absorption and emission operators.[19] A simplification is made by defining the constants $E_{ex,1} \equiv E_n - E_{i,el}$ and $E_{ex,2} \equiv E_m - E_{f,el}$, which can be considered incident and final resonant energies, respectively, and the respective inverse lifetimes $\Gamma_1$ and $\Gamma_2$.[7,19] With this simplification, one ignores the details of the intermediate states. We note that this formula contains separate denominators involving incident and final photon energies. The scattering intensity is given by

$$I \sim L(E_{ex,1} - E_i, \Gamma_1) L(E_{ex,2} - E_f, \Gamma_2)$$
$$\times |\langle f|b_2 H_c b_1|i\rangle|^2 \delta(E_{f,el} - E_{i,el} - \omega), \quad (2)$$

where $L(E, \Gamma_i)$ represents a Lorentzian function with half-width $\Gamma_i$.

To model the shake-up process, we replace $|\langle f|b_2 H_c b_1|i\rangle|^2$ with a sum of Gaussian functions, each representing a distinct symmetry-allowed shake-up excitation with energy $\Delta$ and heuristic inverse lifetime $\Gamma_s$:

$$G(\omega) = \exp\left(-\frac{(\omega - \Delta)^2}{2\Gamma_s^2}\right). \quad (3)$$

The single excitation observed in prior work on $La_2CuO_4$ (Ref. 7) was described with $\Gamma_1 = \Gamma_2 = 2.38$ eV, $E_{ex,1} = E_{ex,2} = 8995$ eV, $\Gamma_s = 3.9$ eV, and $\Delta = 6.1$ eV. Since we have been able to resolve a multiplet of excitations rather than a single excitation, we apply third-order perturbation theory to the entire multiplet. In our calculation, we find that four valence excitations with energies $\Delta = 2.3$, 3, 4 and 7.2 eV are adequate to represent the spectra for both polarization conditions. The result of this calculation is shown in Fig. 9(b). For this particular calculation, $\Gamma_s = 0.4$ 1.0 and 1.1 eV for the lower three excitations, respectively. We find that our data can be adequately represented if the 7.2 eV molecular orbital excitation resonates for transitions into both well- and poorly screened states, with variable characteristics. This excitation is represented by two Gaussians, with $\Gamma_s$ set to 3.9 eV (well screened) and 1.9 eV (poorly screened), and we therefore consider a total of five Gaussians for four excitations.

We note that the 5 eV feature discussed in Secs. III and IV was not considered in the above calculations since it is most prominent at high incident energies and shifts with $E_i$. It therefore seems likely that this feature may actually be associated with a resonance of the 7.2 eV molecular orbital excitation at the well-screened state. Due to the double-resonance denominator, each component may, in principle, show two separate resonances for $E_i = E_{ex,1}$ and $E_f = E_{ex,2}$. For the final-energy resonance, as the incident energy changes, the peak position of the excitation shifts to $\omega_{peak} = E_i - E_{ex,2}$ so as to maintain the same final energy. In the two-dimensional contour plot of Fig. 9, this manifests itself as a slope-1 streak of intensity.

The inverse lifetimes determine the shapes of the resonant spectral features. When $\Gamma_1$, $\Gamma_2$, and $\Gamma_s$ approach the value of excitation energy $\Delta$, the two resonances merge and become indistinguishable. If $\Gamma_1$ or $\Gamma_2$ is small compared to $\Delta$ and $\Gamma_s$, one of the two resonances nearly disappears, and the re-

sponse is either a circular region or a slope-one streak. By carefully choosing $\Gamma_i$ and $E_{ex,i}$ $(i=1,2)$ for each component, we we were able to emulate the main characteristics of the experimental data. As seen from Fig. 9(a), the lowest three excitations are only strongly resonant at the well-screened state, while the 7.2 eV excitation is associated with the poorly screened state. Consequently, $E_{ex}$ should be different for the latter. For the slope-1 streak component, the incident resonance energy is the same as for the lower three excitations, but we find it necessary to choose a slightly smaller $E_{ex,2}$.

For out-of-plane polarization, we set $\Gamma_1=\Gamma_2=2$ eV and $E_{ex,1}=E_{ex,2}=8990$ eV for the lower three excitations. For the 7.2 eV component that results in the diagonal streak, we set $\Gamma_1=1.7$ eV, $\Gamma_2=1.5$ eV, $E_{ex,1}=8990$ eV, and $E_{ex,2}=8989$ eV, and for the other 7.2 eV component we chose $\Gamma_1=1.0$ eV, $\Gamma_2=1.5$ eV, and $E_{ex,1}=E_{ex,2}=8998.5$ eV. For in-plane polarization, we simply shifted all $E_{ex}$ values by 4 eV, and adjusted the relative intensity between the three low-lying excitations and the two 7.2 eV components.

The above analysis has two important implications. One is that the "5 eV" feature is to be viewed as a shake-up excitation at 7.2 eV. The second important implication is that this local molecular-orbital excitation not only resonates at the poorly screened state at which copper has an open-shell configuration ($1\underline{s}3d^9\underline{4p}$), but also at the well-screened state ($1\underline{s}3d^{10}\underline{L}\underline{4p}$). This is different from findings for CuO and from the argument that the observed shake-up excitation requires the $3d^9$ open-shell configuration and should be absent at the well-screened state.[19] However, we note that the molecular-orbital excitation was observed to be resonant at both well-screened and poorly screened states in superconducting $HgBa_2CuO_{4+\delta}$.[12]

We will now discuss a different interpretation for the slope-1 component of the streak of intensity that relates it to a resonant excitation into the continuum of unoccupied states.[45,46] Figure 2 shows the zone-center RIXS spectra together with the respective absorption spectra for both polarization condtions. The RIXS intensity is plotted versus final photon energy ($E_f$) instead of energy transfer ($\omega$). We find that the spectra collapse to a peak, with an envelope of approximately Lorentzian shape, centered at about $E_f=8991$ eV for in-plane polarization and $E_f=8987$ eV for out-of-plane polarization. The peak position lies ~4 eV below the photoabsorption threshold for both polarization conditions. This observation is consistent with the presence of slope-1 streaks in the contour plots for both polarization conditions: for in-plane polarization this streak starts at $E_i \sim 8995$ eV and for out-of-plane polarization it starts at $E_i \sim 8991$ eV.

The photon-absorption process near the Cu $K$ edge is comprised of transitions to either narrow molecular orbitals or continuum unoccupied states. For discrete levels, such as the well-screened and poorly screened states, induced valence excitations resonate and follow the Raman-Stokes law as $E_i$ crosses the discrete levels, i.e., the excitation energies $\Delta$ do not vary with incident photon energy. On the other hand, a resonance due to transitions to continuum states behaves differently. Here, the resonance condition is fulfilled for every incident energy tuned to the continuum, and the subsequent emission is independent of $E_i$ once the incident energy increases above the lower edge of the continuum. When $E_i$ is below the edge, the resonant emission should also follow the Raman-Stokes behavior, but the spectral weight may be suppressed due to the small density of states below the edge. Our observation is consistent with the existence of a continuous unoccupied band of $4p$ symmetry, with an edge at ~8991 and ~8995 eV for the respective polarizations, and a width of about 3–4 eV. This would support the view that a combination of an extended picture of itinerant $4p$ electrons and of localized molecular orbitals is necessary to interpret the $K$-edge absorption spectra[21] and the nature of the intermediate states in RIXS.

We note that the envelope of the in-plane data collapse shown in Fig. 2(a) is very similar in shape and position to the XAS corresponding to the well-screened state for out-of-plane polarization [Fig. 2(b)]. This leads us to a third interpretation of the slope-one contribution to the RIXS cross section shown in Fig. 9(a). Specifically, it suggests that part of the in-plane-polarized RIXS signal can be interpreted through the following complex dynamical process illustrated in Fig. 8: $La_2CuO_4$ absorbs a photon of energy $E_i \sim 8995$ eV with polarization $\mathbf{E} \perp c$, creating on a Cu site a well-screened $1s$ core hole and an electron in a $4p_\sigma$ orbital [Fig. 8(b)]. The $4p_\sigma$ electron then evolves into a $4p_z$ state [Fig. 8(c)] via a subsequent relaxation process. Finally, the $4p_z$ electron recombines with the $1s$ core hole, emitting a photon with energy ~8991 eV. However, for out-of-plane polarization, electrons are already excited into a $4p_z$ state, and this relaxation will not occur. Nevertheless, the envelope for out-of-plane polarization lies also 4 eV below that of the main edge. This interpretation therefore requires the existence of a discrete lower-energy state with energy 8987 eV for $4p_z$ electron to relax into. Interestingly, in Ref. 7, a resonance of approximately this energy was observed with in-plane polarization. Further experimentation combined with theoretical modeling can be expected to resolve the origin of the slope-1 streak of intensity.

## VI. SUMMARY

In summary, we have presented a detailed Cu $K$-edge RIXS study of $La_2CuO_4$ in which we resolve a multiplet of charge-transfer excitations in the 1–7 eV range. We suggest several interpretations to explain the polarization-dependent spectra. A calculation applying third-order perturbation theory introduces a final-energy resonance and successfully simulates the main characteristics of the spectra for both polarization conditions. On the other hand, transitions to a continuum of $4p$ bands that begins at the main absorption edge as well as $4p_\sigma \rightarrow 4p_z$ relaxation are offered as alternative explanations to the fluorescence-like component in the contours. These proposals all emphasize the important role of the $4p$ electrons in the RIXS cross section.

## ACKNOWLEDGMENTS

The authors gratefully acknowledge valuable discussions with P. Abbamonte, U. Bergmann, J. van den Brink,

T. P. Devereaux, M. V. Klein, Y. J. Kim, K.-W. Lee, R. S. Markiewicz, W. E. Pickett, K. M. Shen, Z. X. Shen, M. van Veenendaal, and F. C. Zhang. The work at Stanford University was supported by the DOE under Contract No. DE-AC02-76SF00515 and by the NSF under Grant No. 0405655. Work at the CMC-XOR beamlines is supported in part by the Office of Basic Energy Sciences of the U.S. Department of Energy and by the National Science Foundation Division of Materials Research. Use of the Advanced Photon Source is supported by the Office of Basic Energy Sciences of the U.S. Department of Energy under Contract No. W-31-109-Eng-38.

[1] C. A. Burns, P. Abbamonte, E. D. Isaacs, and P. M. Platzman, Phys. Rev. Lett. **83**, 2390 (1999).
[2] C. Dallera, M. Grioni, A. Shukla, G. Vanko, J. L. Sarrao, J. P. Rueff, and D. L. Cox, Phys. Rev. Lett. **88**, 196403 (2002).
[3] P. Wernet, D. Nordlund, U. Bergmann, M. Cavalleri, M. Odelius, H. Ogasawara, L. A. Naslund, T. K. Hirsch, L. Ojamae, P. Glatzel, L. G. M. Pettersson, and A. Nilsson, Science **304**, 995 (2004).
[4] F. Sette, G. Ruocco, M. Krisch, U. Bergmann, C. Masciovecchio, V. Mazzacurati, G. Signorelli, and R. Verbeni, Phys. Rev. Lett. **75**, 850 (1995).
[5] M. d'Astuto, P. K. Mang, P. Giura, A. Shukla, P. Ghigna, A. Mirone, M. Braden, M. Greven, M. Krisch, and F. Sette, Phys. Rev. Lett. **88**, 167002 (2002).
[6] J. P. Hill, C. C. Kao, W. A. L. Caliebe, M. Matsubara, A. Kotani, J. L. Peng, and R. L. Greene, Phys. Rev. Lett. **80**, 4967 (1998).
[7] P. Abbamonte, C. A. Burns, E. D. Isaacs, P. M. Platzman, L. L. Miller, S. W. Cheong, and M. V. Klein, Phys. Rev. Lett. **83**, 860 (1999).
[8] K. Hämäläinen, J. P. Hill, S. Huotari, C. C. Kao, L. E. Berman, A. Kotani, T. Ide, J. L. Peng, and R. L. Greene, Phys. Rev. B **61**, 1836 (2000).
[9] M. Z. Hasan, E. D. Isaacs, Z. X. Shen, L. L. Miller, K. Tsutsui, T. Tohyama, and S. Maekawa, Science **288**, 1811 (2000).
[10] Y. J. Kim, J. P. Hill, C. A. Burns, S. Wakimoto, R. J. Birgeneau, D. Casa, T. Gog, and C. T. Venkataraman, Phys. Rev. Lett. **89**, 177003 (2002).
[11] Y. J. Kim, J. P. Hill, S. Komiya, Y. Ando, D. Casa, T. Gog, and C. T. Venkataraman, Phys. Rev. B **70**, 094524 (2004).
[12] L. Lu, X. Zhao, J. N. Hancock, G. Chabot-Couture, N. Kaneko, O. P. Vajk, G. Yu, S. Grenier, Y. J. Kim, D. Casa, T. Gog, and M. Greven, Phys. Rev. Lett. **95**, 217003 (2005).
[13] K. Ishii, K. Tsutsui, Y. Endoh, T. Tohyama, S. Maekawa, M. Hoesch, K. Kuzushita, M. Tsubota, T. Inami, J. Mizuki, Y. Murakami, and K. Yamada, Phys. Rev. Lett. **94**, 207003 (2005).
[14] K. Ishii, K. Tsutsui, Y. Endoh, T. Tohyama, K. Kuzushita, T. Inami, K. Ohwada, S. Maekawa, T. Masui, S. Tajima, Y. Murakami, and J. Mizuki, Phys. Rev. Lett. **94**, 187002 (2005).
[15] K. Ishii, T. Inami, K. Ohwada, K. Kuzushita, J. Mizuki, Y. Murakami, S. Ishihara, Y. Endoh, S. Maekawa, K. Hirota, and Y. Moritomo, Phys. Rev. B **70**, 224437 (2004).
[16] S. Grenier, J. P. Hill, V. Kiryukhin, W. Ku, Y. J. Kim, K. J. Thomas, S. W. Cheong, Y. Tokura, Y. Tomioka, D. Casa, and T. Gog, Phys. Rev. Lett. **94**, 047203 (2005).
[17] C. C. Kao, W. A. L. Caliebe, J. B. Hastings, and J. M. Gillet, Phys. Rev. B **54**, 16361 (1996).
[18] M. H. Krisch, C. C. Kao, F. Sette, W. A. Caliebe, K. Hämäläinen, and J. B. Hastings, Phys. Rev. Lett. **74**, 4931 (1995).
[19] G. Döring, C. Sternemann, A. Kaprolat, A. Mattila, K. Hämäläinen, and W. Schulke, Phys. Rev. B **70**, 085115 (2004).
[20] P. Glatzel and U. Bergmann, Coord. Chem. Rev. **249**, 65 (2005a).
[21] J. M. Tranquada, S. M. Heald, W. Kunnmann, A. R. Moodenbaugh, S. L. Qiu, Y. W. Xu, and P. K. Davies, Phys. Rev. B **44**, 5176 (1991).
[22] A. Kotani and S. Shin, Rev. Mod. Phys. **73**, 203 (2001).
[23] E. Collart, A. Shukla, J. P. Rueff, P. Leininger, H. Ishii, I. Jarrige, Y. Q. Cai, S. W. Cheong, and G. Dhalenne, Phys. Rev. Lett. **96**, 157004 (2006).
[24] R. J. Birgeneau, M. Greven, M. A. Kastner, Y. S. Lee, B. O. Wells, Y. Endoh, K. Yamada, and G. Shirane, Phys. Rev. B **59**, 13788 (1999).
[25] O. P. Vajk, P. K. Mang, M. Greven, P. M. Gehring, and J. W. Lynn, Science **295**, 1691 (2002).
[26] S. M. Heald, J. M. Tranquada, A. R. Moodenbaugh, and Y. W. Xu, Phys. Rev. B **38**, 761 (1988).
[27] K.-W. Lee and W. E. Pickett (private communication).
[28] Y. J. Kim (private communication).
[29] P. Glatzel and U. Bergmann, Coord. Chem. Rev. **249**, 65 (2005b).
[30] G. D. Mahan, *Many-Particle Physics* (Springer-Verlag, New York, 2000).
[31] F. deGroot, Chem. Rev. (Washington, D.C.) **101**, 1779 (2001).
[32] T. Nomura and J. I. Igarashi, Phys. Rev. B **71**, 035110 (2005).
[33] K. Tsutsui, T. Tohyama, and S. Maekawa, Phys. Rev. Lett. **91**, 117001 (2003).
[34] F. C. Zhang and T. M. Rice, Phys. Rev. B **37**, 3759 (1988).
[35] F. C. Zhang and K. K. Ng, Phys. Rev. B **58**, 13520 (1998).
[36] A. S. Moskvin, R. Neudert, M. Knupfer, J. Fink, and R. Hayn, Phys. Rev. B **65**, 180512(R) (2002).
[37] H. Tolentino, M. Medarde, A. Fontaine, F. Baudelet, E. Dartyge, D. Guay, and G. Tourillon, Phys. Rev. B **45**, 8091 (1992).
[38] B. O. Wells, Z. X. Shen, A. Matsuura, D. M. King, M. A. Kastner, M. Greven, and R. J. Birgeneau, Phys. Rev. Lett. **74**, 964 (1995).
[39] C. Dürr, S. Legner, R. Hayn, S. V. Borisenko, Z. Hu, A. Theresiak, M. Knupfer, M. S. Golden, J. Fink, F. Ronning, Z.-X. Shen, H. Eisaki, S. Uchida, C. Janowitz, R. Müller, R. L. Johnson, K. Rossnagel, L. Kipp, and G. Reichardt, Phys. Rev. B **63**, 014505 (2000).
[40] F. Ronning, C. Kim, K. M. Shen, N. P. Armitage, A. Damascelli, D. H. Lu, D. L. Feng, Z.-X. Shen, L. L. Miller, Y. J. Kim, F. Chou, and I. Terasaki, Phys. Rev. B **67**, 035113 (2003).
[41] K. H. Ahn, A. J. Fedro, and M. van Veenendaal, cond-mat/0412635 (unpublished).
[42] R. S. Markiewicz and A. Bansil, Phys. Rev. Lett. **96**, 107005 (2006).
[43] H. Eskes and G. A. Sawatzky, Phys. Rev. B **44**, 9656 (1991).
[44] P. M. Platzman and E. D. Isaacs, Phys. Rev. B **57**, 11107 (1998).
[45] F. Gel'mukhanov and H. Ågren, Phys. Rev. B **57**, 2780 (1998).
[46] F. Gel'Mukhanov and H. Ågren, Phys. Rep. **312**, 87 (1999).